Electrochemical Surface Plasmon Resonance and Waveguide-Enhanced Glucose Biosensing with N-Alkylaminated Polypyrrole/Glucose Oxidase Multilayers

Akira Baba,[†,‡] Prasad Taranekar,[†] Ramakrishna R. Ponnapati,[†] Wolfgang Knoll,[§] and Rigoberto C. Advincula*[,†]

Department of Chemistry and Department of Chemical Engineering, University of Houston, Houston, Texas 77204, and Austrian Institute of Technology (AIT) GmbH, Donau-City-Strasse 1, Vienna, Austria 1220

ABSTRACT In this work, we report an electrochemical surface plasmon resonance/waveguide (EC-SPR/waveguide) glucose biosensor that could detect enzymatic reactions in a conducting polymer/glucose oxidase (GO_x) multilayer thin film. In order to achieve a controlled enzyme electrode and waveguide mode, GO_x (negatively charged) was immobilized with a water-soluble, conducting N-alkylaminated polypyrrole (positively charged) using the layer-by-layer (LbL) electrostatic self-assembly technique. The electrochemical and optical signals were simultaneously obtained from the composite LbL enzyme electrode upon the addition of glucose as mediated by the electroactivity and electrochromic property of the polypyrrole layers. Signal enhancement in EC-SPR detection is obtained by monitoring the doping−dedoping events on the polypyrrole. The real-time optical signal could be distinguished between the change in the dielectric constant of the enzyme layer and other nonenzymatic reaction events such as adsorption of glucose and the change of the refractive index of the solution. This was possible by correlation of both the SPR mode and the $m = 0$ and 1 modes of the waveguide in an SPR/waveguide spectroscopy experiment.

KEYWORDS: surface plasmon • glucose • biosensor • conducting polymer • enzyme • waveguide

INTRODUCTION

Electrically conducting and π-conjugated polymers have been shown to be highly sensitive materials for monitoring and mediating enzymatic interactions. This is attributed to the high conductivity and specific electrochemical redox properties of conducting polymers, which can be paired with redox events present in enzymatic reactions (1−3). For example, the redox property of conducting polymers changes upon reduction of the enzyme glucose oxidase (GO_x). This change can then be detected as either an electrochemical signal or an optical signal. Upon the introduction of glucose, glucose oxidase is reduced and glucose converted to gluconic acid (gluconolactone). In conventional glucose sensors without conducting polymer mediators, the reduced glucose oxidase drives the conversion of O_2 to H_2O_2, in the presence of O_2. H_2O_2 can then undergo oxidation to give H_2O. On the other hand, in the case of conducting polymer mediators, the oxidation of a reduced chemical species/polymer material can be directly measured by an electrode surface (see SI Figure 1 in the Supporting Information). Thus, electroactive conducting polymers can be considered as "wiring" materials for the electrochemical activation of redox enzymes (4). Redox enzymes usually have poor direct electrical conductivity contact and communication with metallic electrodes. An electroactive conducting polymer provides the matrix for electron transfer from the enzyme to the electrode, correlated with changes in the electrochemical (I−V) signal.

The surface plasmon resonance (SPR) optical technique is a powerful tool for characterizing the dielectric properties of surfaces, interfaces, and thin films. In biosensor applications, this technique allows for the investigation of biomolecular adsorption/desorption events at surfaces and provides in situ time-dependent surface coverage measurements without the need for labeling. We have previously demonstrated the electrochemical-SPR (EC-SPR) technique for characterization of conducting polymer thin films including polyaniline, poly(3,4-ethylenedioxythiophene) (PEDOT), poly(vinylcarbazole), and polythiophenes (5−9). In EC-SPR measurements, the gold substrate that carries the optical surface mode is simultaneously used as the working electrode in a standard three-electrode electrochemical experiment. One of the advantages in using the EC-SPR technique is that the electrochemical and optical properties are simultaneously obtained on surfaces and ultrathin films at the nanometer scale. This involves the in situ monitoring of the film thickness and electrochromic properties during the anion doping/dedoping process of deposited conducting polymers. More recently, we have demonstrated the in situ EC-SPR-atomic force microscopy (EC-SPS-AFM) technique for "real-time"

* To whom correspondence should be addressed. E-mail: radvincula@uh.edu.
Received for review April 28, 2010 and accepted July 19, 2010
† University of Houston.
‡ Current address: Center for Transdisciplinary Research, Niigata University, Niigata 950-2181, Japan.
§ AIT GmbH.
DOI: 10.1021/am100373v

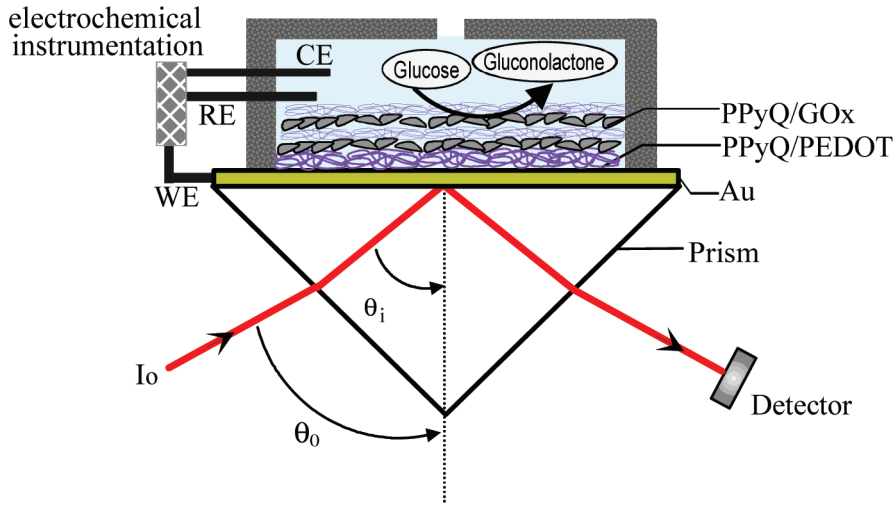

FIGURE 1. EC-SPR glucose biosensor schematic diagram in a Kretschmann configuration with a three-electrode cell setup.

Scheme 1. Synthesis Scheme for the Water-Soluble Polypyrrole PPY-Q

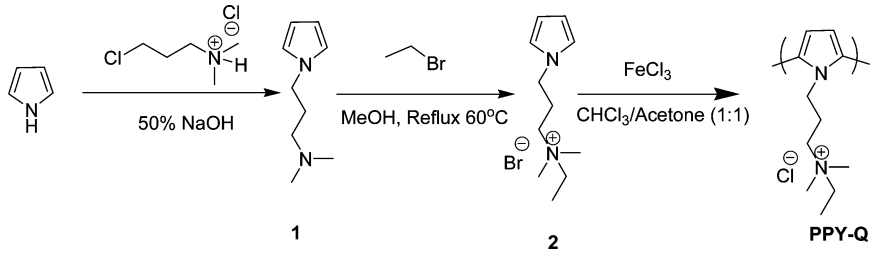

dynamic and simultaneous acquisition of the dielectric (optical), surface morphological, and electrochemical data of a depositing conducting polymer thin film at the electrode/electrolyte interface (10). This enabled differentiation of cyclic voltammetry (CV) and potentiostatically (chronoamperometrically) deposited films between their dielectric, electrochemical, and morphological properties in real time.

However, there are not too many examples of laser-excited evanescent-wave SPR techniques for glucose sensing (11), as compared to the quartz crystal microbalance (QCM) or EC-QCM techniques (12). One of the reasons for this is that for SPR it is not easy to distinguish between changes in the thickness, dielectric constant of the layer, adsorption of glucose, and refractive index change of the buffer; i.e., the real-time event is sensitive to both enzymatic and nonenzymatic reactions (13). Another is the poor stability of the composite conducting polymer/GO_x enzyme film that is prepared in situ (17). This has been commonly done by direct in situ anodic pyrrole electropolymerization with GO_x at the electrode surface (16). In this work, we have endeavored to apply a combined EC-SPR and waveguide approach (Figure 1) to enable better differentiation of these factors. First, a water-soluble, positively charged N-alkylaminated polypyrrole was synthesized for pairing with the negatively charged GO_x. The composite enzyme electrode was fabricated by the assembly of polypyrrole and GO_x via the layer-by-layer (LbL) electrostatic self-assembly technique (14, 20). Compared to the as-deposited LbL film, it was observed that enhancement in the sensitivity for an SPR/amperometric sensor can be achieved by taking advantage of the doping−dedoping properties of these films in a neutral buffer solution condition. Because the LbL film can be homogeneously assembled, dips from both SPR and waveguide were obtained when thicker films were fabricated. Through measurement using the $m = 0$ and 1 modes in an SPR/waveguide spectroscopy experiment, we were able to separate the signal specific only to the GO_x enzymatic activity via changes in the dielectric constant. Compared to QCM measurements, this setup allows one to distinguish contribution of the GO_x enzymatic activity from nonspecific adsorption and/or changes in the subphase dielectric constant (12). Thus, we have harnessed the EC-SPR and waveguide techniques for demonstrating a glucose biosensor with possible applications for other enzymatic biological optoelectronic differentiation.

EXPERIMENTAL DETAILS

Materials. Glucose oxidase (GO_x, from *Aspergillus niger*) was obtained from Aldrich and used immediately. Scheme 1 illustrates the synthesis route for the water-soluble polypyrrole (PPY-Q) or poly[*N*,*N*-dimethylethyl-3-(1*H*-pyrrol-1-yl)propane-1-ammonium chloride]. The compound **2**, which is a precursor for the synthesis of PPY-Q, was also found to be water-soluble. The synthetic details and characterization data are mentioned in the Supporting Information, and the procedure was previously reported elsewhere (15). The polymer PPY-Q was also found to be soluble in organic solvents such as acetone, tetrahydrofuran, dimethyl sulfoxide, and *N*,*N*-dimethylformamide. The PEDOT:poly(styrene sulfonate) (PSS) aqueous solution was made by mixing 50 mL of Milli-Q water and 5 mL of a PEDOT:PSS colloidal suspension (available from BAYTRON P, Bayer Corp.) after filtration using a syringe-driven filter "Millex" with diameter 0.70 μm (Millipore). A poly(diallyldimethylammonium

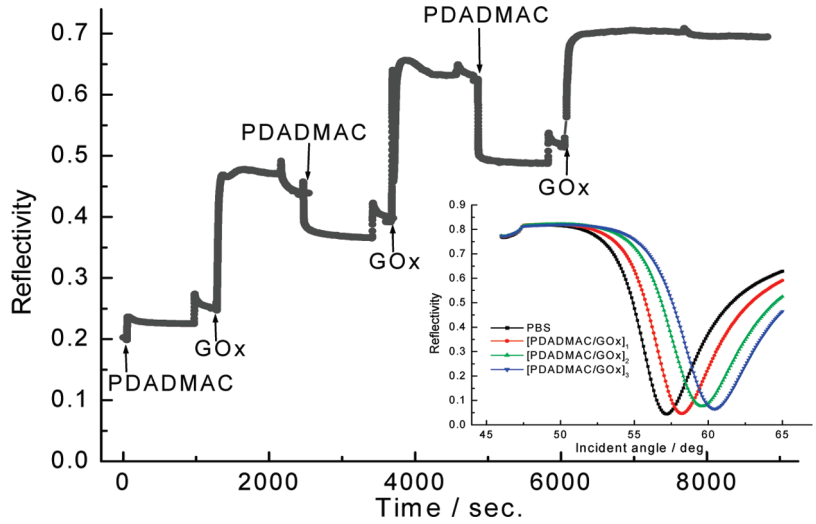

FIGURE 2. SPR kinetic curve and angular scans during LBL deposition. Inset: reflectivity−angular scan for each deposited layer.

chloride) (PDADMAC; from Aldrich) solution was prepared using Milli-Q water with a concentration of 2 mg/mL. 3-Mercapto-1-propanesulfonic sodium was also obtained from Aldrich and used as received. Adsorption and sensing was done on a phosphate-buffered saline (PBS) at pH ∼ 7, a water-based salt solution containing sodium chloride, sodium phosphate, and/or potassium chloride and potassium phosphate.

LbL Adsorption. LbL adsorption of the polyanion and polycation was performed following the popular multilayer electrostatic deposition approach (16, 17). The gold surface of the flat solid substrate was functionalized by immersing the slide for 90 min in an ethanol solution of a 3-mercapto-1-propanesulfonic sodium salt (0.2 mg/mL) (followed by rinsing), creating a uniformly charged (negative) substrate surface. The gold film with a thickness of ca. 50 nm was deposited by vacuum evaporation onto an LaSFN9 glass slide. The gold/glass or glass substrates with functionalized surfaces were alternately immersed for 15 min in PBS at pH ∼ 7 and buffer solutions of the polycation and polyanion (or glucose oxidase) until the desired number of layers was achieved. Glucose oxidase was stored in a refrigerator at 4 °C and used immediately for LbL fabrications for the EC-SPR experiment. For EC-SPR/waveguide experiments, glucose oxidase was used at 25 °C, and the immersion time was increased by up to several hours. Rinsing with PBS (pH 7.4) was done between depositions.

Electrochemical Measurement. Electrochemical experiments were performed in a conventional three-electrode cell with the gold/glass substrate as the working electrode, a platinum wire as the counter electrode, and an Ag/AgCl (3 M NaCl) reference electrode. A potentiostat (PARSTAT 2263A, Princeton Applied Research) was used for the CV or amperometric biosensor experiments.

EC-SPR. Figure 1 shows the attenuated total reflection (ATR) setup used for excitation of surface plasmons in the Kretschmann configuration combined with an electrochemical cell. A triangular LaSFN9 prism was used (17). The gold/glass substrates were clamped against the Teflon cell with an O-ring, providing a liquid-tight seal. The Teflon cell was then mounted to the 2-axis goniometer for investigations by SPR. Surface plasmons were excited at the metal−dielectric interface, upon total internal reflection of a p-polarized laser light beam. A He−Ne laser ($\lambda = 632.8$ nm) was used in all measurements. The optical/electrochemical processes on gold were detected by monitoring the reflectivity either as a function of the incident angle θ_0 or at a fixed incident angle. The *WINSPALL* program was used for modeling (thickness and dielectric constant determination).

RESULTS AND DISCUSSION

Fabrication of the LbL Film. In order to fabricate a controlled enzyme electrode and to investigate the sensing properties without conducting polymers, GO_x(−) was first immobilized with the nonelectrically conducting PDADMAC(+) polyelectrolyte using the LbL technique. Figure 2 shows the reflectivity change measured in situ by SPR during the multilayer fabrication process. The inset shows angular scans taken after deposition of each bilayer. As shown in this figure, a monotonous reflectivity increase with an increase in the number of layers indicates a regular and step deposition of PDADMAC/GO_x layers. One can see that for each bilayer the reflectivity change caused by GO_x is much larger than that of PDADMAC, indicating a larger amount of deposition of GO_x. The decrease of reflectivity during the deposition process of PDADMAC indicates some amount of desorption of GO_x during this process. The thickness obtained by Fresnel modeling is 1 nm for PDADMAC and 9 nm for GO_x.

The conducting polymer/enzyme electrode was then fabricated for optimum electroactivity (see also SI Figure 2 in the Supporting Information). In this case, it was necessary to first deposit PPy-Q(+) and PEDOT:PSS(−) layers on the gold electrode in order to enhance the electron transfer between glucose and the gold electrode. Figure 3 shows deposition of 5.5 bilayers of PPy-Q and PEDOT:PSS, followed by deposition of 2 bilayers of PPy-Q and GO_x in PBS. The inset shows the angular scan taken before and after the entire deposition. A linear increase of the reflectivity was observed, which indicates homogeneous deposition for the PPy-Q/PEDOT:PSS bilayer system (2.3 nm thickness/bilayer). Although some amount of desorption of GO_x was again observed during deposition of PPy-Q, a more linear increase of PPy-Q/GO_x was also observed. One can see that the reflectivity is stable after each deposition of PPy-Q/GO_x (∼6 nm thickness) pairs, indicating that stable immobilization of GO_x was essentially obtained with the conducting polymers using the LbL deposition technique.

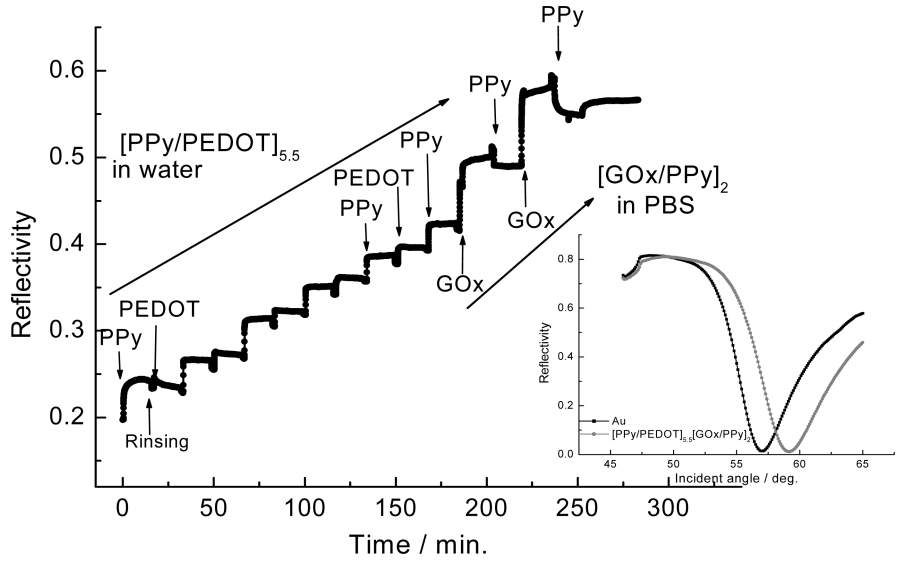

FIGURE 3. SPR kinetic curve and angular scan during LBL deposition of the composite layers. Inset: reflectivity−angular scan for each deposited layer.

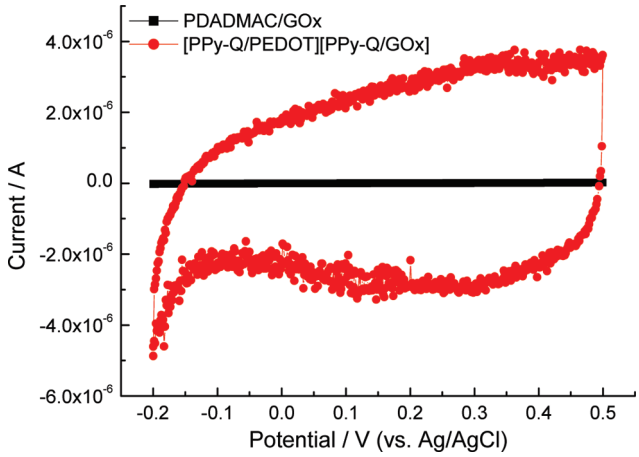

FIGURE 4. CV of functionalized gold electrodes with two different LbL film compositions.

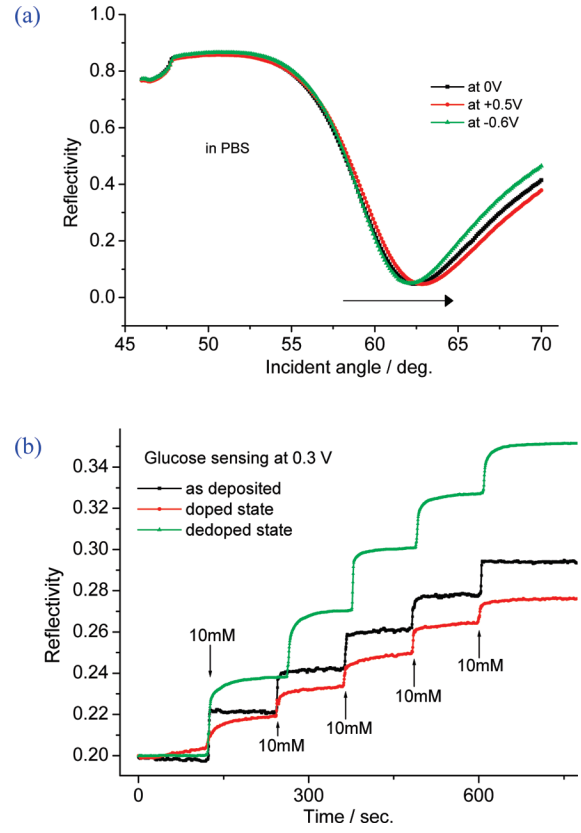

FIGURE 5. (a) SPR angular−reflectivity curves of a PPy-Q/PEDOT:PPSS-PPy-Q/GO$_x$ film at different applied potentials. (b) SPR glucose sensing as a function of the concentration (time) at different doping states.

The electroactivity between the two films was then compared in an electrolyte buffer solution, and the doping−dedoping events were monitored. In principle, the electroactivity should involve a current increase or decrease with CV scanning, indicating the transport of ions and electron transfer (see SI Figure 3 in the Supporting Information). Figure 4 shows the cyclic voltammograms of the PDADMAC/GO$_x$-functionalized electrode and PPy-Q/PEDOT:PPSS-PPy-Q/GO$_x$-functionalized electrode in PBS (pH 7.4) between −0.2 and +0.5 V. As shown in this figure, the PPy-Q/PEDOT:PSS- and PPy-Q/GO$_x$-functionalized electrode showed a good current cycle (electroactivity) in PBS, while PDADMAC/GO$_x$ showed little current change in this region. This indicates that the conducting polymer/glucose oxidase electrode can be used at a low potential in a neutral solution. It is very important to operate glucose sensing at potentials lower than 0.3 V in order to exclude the possibility of nonenzymatic oxidation of glucose and oxidation of other analytes such as acetaminophen, ascorbic acid, and uric acid (18). These other analytes can be present in real samples, e.g., blood or urine, for laboratory analysis. It should be noted that glucose sensing at 0.3 V is also not affected by hydrogen peroxide, which depends on the residual oxygen in the cell (4). The SPR reflectivity curves of a PEDOT film prepared at constant potentials, i.e., 0, −0.6, and +0.5 V, are shown in Figure 5a. These shifts in reflectivity are important because it highlights the electrochromic properties of the deposited PPy-Q/GO$_x$ films. The angular measurements at each potential were performed 2.5 min after the

potential was changed in a neutral solution. The resonance angle of the SPR curves repeatedly changed on going from the doped state to the dedoped state of the polymer film and from the dedoped state to the doped state stability and reproducibility.

EC-SPR Experiments for Detection of Glucose. Because the electrochromic property was obtained in a neutral solution, it should be possible to carry out glucose sensing after doping and dedoping and at the as-deposited states, as shown in Figure 5b. The sensing was carried out in a neutral PBS buffer upon the addition of 10 mM glucose every 5 min. As shown in this figure, the degree of optical signal change is dependent on the doped/dedoped state film before sensing. From these results, one can see that the doped/dedoped state did not move back even when the potential was set at 0.3 V during the sensing experiment. This is probably because the ions are more difficult to diffuse out of the LbL films in a PBS solution. Furthermore, this result indicates that the dedoped state has the highest reflectivity change or is more sensitive for the optical signal. This is not counterintuitive because the polypyrrole film is oxidized in the glucose sensing (reduction) event and thus the dedoped state shows the highest change, i.e., from a dedoped state to a more doped state (11, 12). The results obtained also highlight the fact that the change of reflectivity can also be controlled by the doping state of the conducting polymer films. It should be noted that the magnitude of this shift is also a function of the electrochromic behavior of the films and the wavelength of the light source for the ATR experiment (19).

Figure 6 shows plots of the simultaneous SPR/amperometric glucose sensing. As explained, the dedoped state showed the highest reflectivity change. In the case of amperometric sensing, the dedoped and as-deposited states showed a smaller change in the current, while the doped state showed a very large change in the current, i.e., micrometer ampere. This is because the LbL film at the doped state facilitates better electron transfer from the glucose to the electrode. The sensitivity of the doped state was 0.3 μA/10 mM, while that of the as-deposited state was 2.8 nA/10 mM. This means that the doping state can have a big advantage over the chosen transduction method for sensing and that amperometric and SPR sensing methods are complementary to each other.

EC-SPR/Waveguide Experiments for Detection of Glucose. Although much enhancement in the current was obtained by doping, the SPR signal still includes the component of the refractive index change of the solution with the addition of glucose. We were able to overcome this problem by utilizing an SPR/waveguide spectroscopy setup (19). Figure 7 shows the simulations of the SPR/waveguide mode on assumptions of a refractive index change of the buffer (a), adsorption of glucose (b), a thickness change of the PPy/GO_x layer (c), and a dielectric constant change of the PPy/GO_x layer (d). In this simulation, the thickness of the PPy/GO_x layer was assumed to be 500 nm (waveguiding). As shown in this figure, the minimum angle of the waveguide

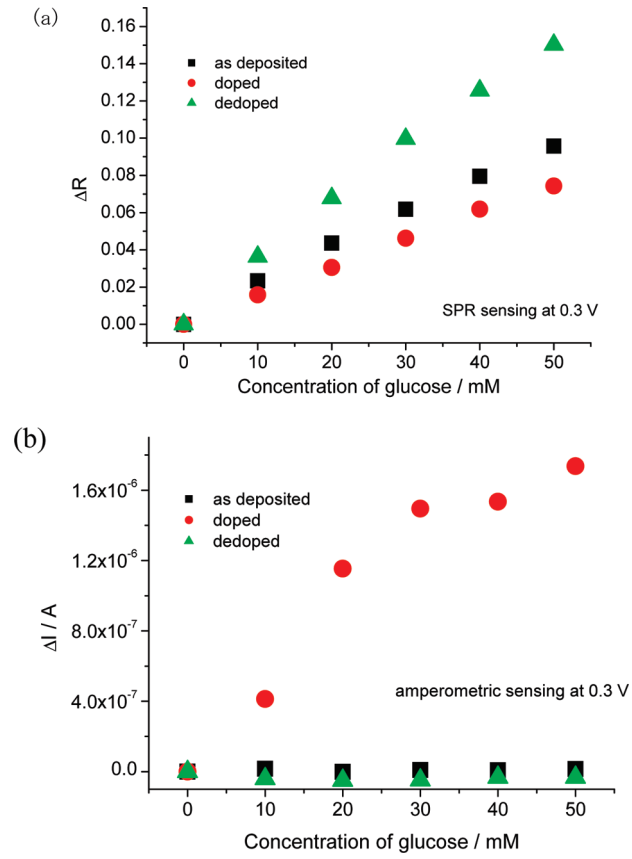

FIGURE 6. Plot of amperometric vs SPR sensing with an increase in the concentration of glucose.

mode ($m = 1$ mode) shifts to higher angle in all cases. On the other hand, in the case of the surface plasmon mode ($m = 0$ mode), the minimum angle shifts only to higher angle in the case of a direct dielectric constant change of the PPy/GO_x layer. This is because the evanescent field of the surface plasmon (~150 nm) is inside the PPy/GO_x layer, such that the curve does not depend on the PPy/GO_x surface adsorption of glucose, the thickness change of the PPy/GO_x layer, and the refractive index of the buffer. Because the enzymatic reaction is generated upon the addition of glucose, GO_x and PPy are reduced because of the electron-transfer event. Hence, the signal can be detected as a change of the dielectric constant of the PPy/GO_x layer. If the waveguide mode produces changes, then this correspondingly includes changes in the thickness of the film. This simulation shows that the SPR/waveguide mode can exclude the possibility of the signal change due to nonenzymatic reactions or simple analyte adsorption (nonspecific) if needed. The reflectivity versus parameter plots in SI Figure 4 in the Supporting Information further highlight the fact that changes in the SPR mode can only be due to the dielectric changes caused by the enzymatic activity. This is very important for real glucose sensing because blood plasma can contain not only glucose but also ascorbic acid, uric acid, acetaminophen, and other potential interfering analytes. Also, blood plasma can have substantially different refractive indexes depending on a person's physiological or disease condition.

To demonstrate the simulated waveguiding principles, actual thick films >500 nm of the composite sensing ele-

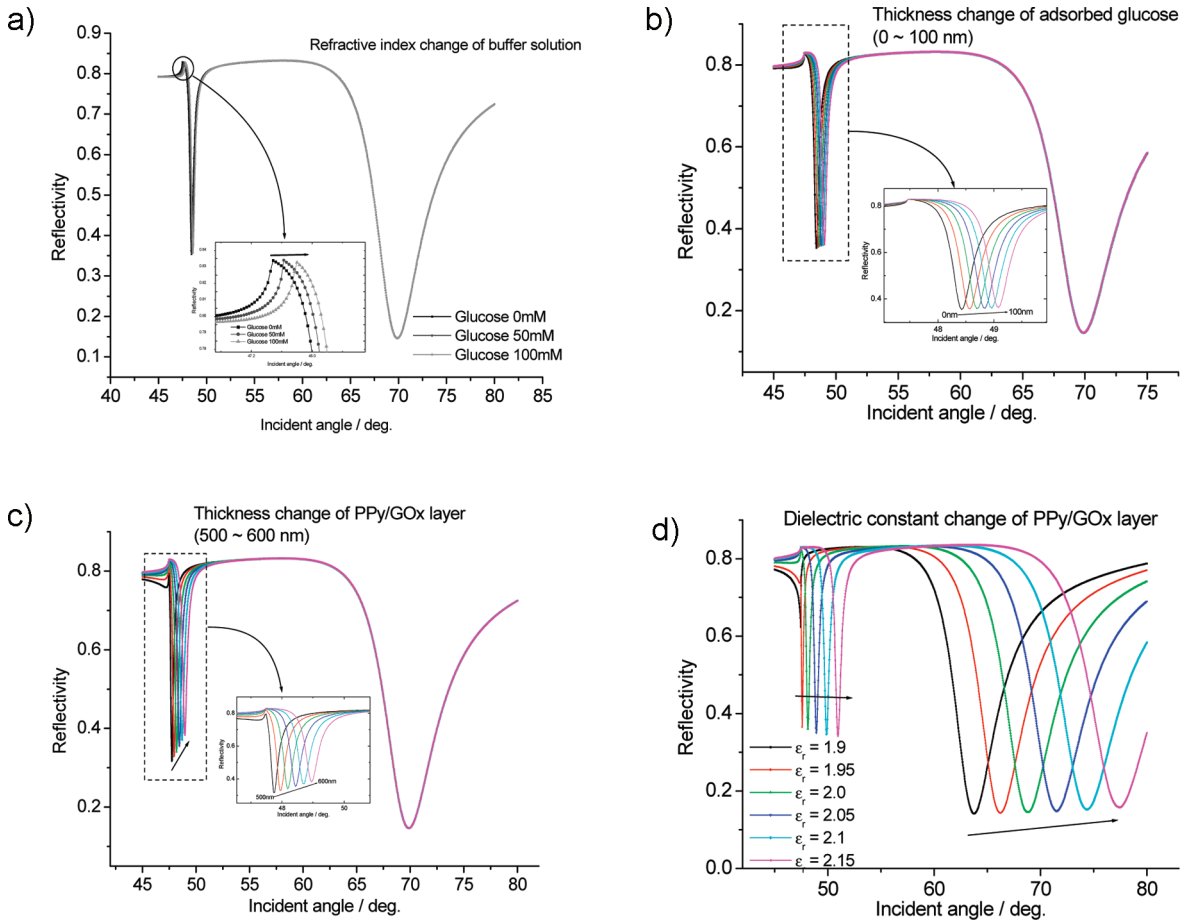

FIGURE 7. Simulation of the SPR/waveguide mode with glucose addition in various parameters: (a) refractive index change of the buffer solution; (b) thickness change of the absorbed glucose; (c) thickness change of the PPy/GO_x layer; (d) dielectric constant change of the PPy/GO_x layer.

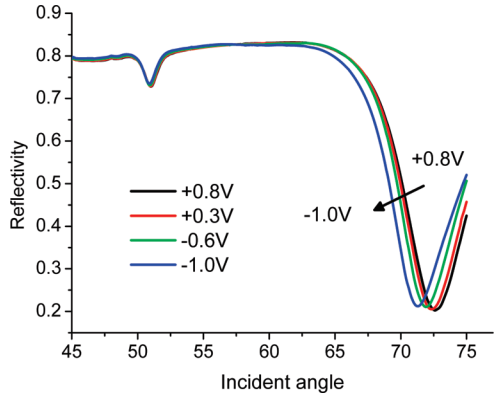

FIGURE 8. Reflectivity angular scan of PPyPEDOT-PPyGO$_x$ on an SPR/waveguide combined mode at various potentials.

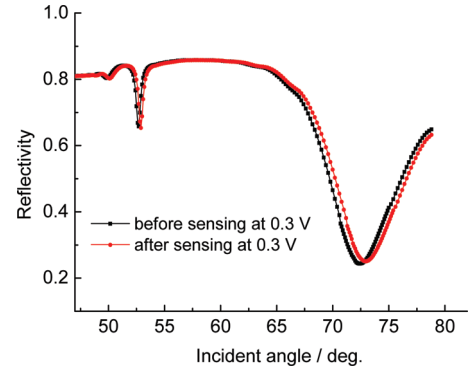

FIGURE 9. Angular SPR curves before and after sensing of glucose at 0.3 V and 10 mM concentration.

ments were fabricated. Figure 8 shows the reflectivity angular curves for 25 bilayers of PPyPEDOT-PPyGO$_x$ LbL films in a PBS solution at several constant potentials. As shown in this figure, both the SPR ($m = 0$) and waveguide ($m = 1$) modes were clearly observed. Because the waveguide can be excited only with a uniform and smooth surface coverage, this indicated that the PPy/LbL film is smooth and formed an ordered structure suitable as a mediator for EC-SPR/waveguide glucose sensing. The SPR dip was sensitively moved toward lower angles when the potential was lower (more negative), while the waveguide mode was almost constant. On the basis of the model calculations shown in Figure 7, this indicates that the dielectric constant of the LbL film is lowered with a decrease in the potential (more negative), while the thickness of the film remained constant at each potential. The lowering of the dielectric potential is a result of the dedoping of the conducting polymer layer because no glucose has yet been introduced. This indicates that the information of the dielectric constant and thickness can indeed be separated using this protocol.

Figure 9 shows the reflectivity–angular scan for 25 bilayers of PEDOT/PPy-PPyGO$_x$ LbL films before and after sensing with 10 mM glucose. As shown in this figure, both

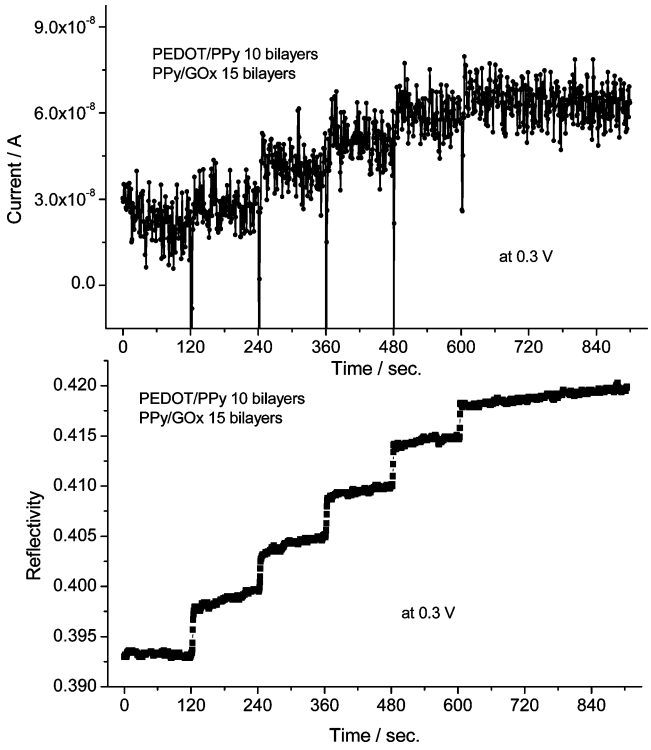

FIGURE 10. Simultaneous observation of the current (above) and SPR reflectivity (below) upon the incremental addition of glucose.

the SPR and waveguide modes were clearly observed and shifted. The SPR minimum angle, $m = 0$, and the waveguide mode, $m = 1$, shifted to a slightly higher angle after the addition of glucose at 0.3 V. First of all, this indicated that the enzyme showed high activity with the addition of glucose within the PPY matrix. The shift in evanescent optical properties (dielectric constant) of the SPR mode is a consequence of a change in the electrochemical activity of PPY present with the GO_x/glucose enzymatic activity. The dielectric change followed digestion of the glucose substrate by the GO_x enzyme. This can be explained by an increase in the dielectric constant as a function of the increased oxidation state of the conducting polymer with the formation of gluconate species. The thickness increase can be attributed to the incorporation of glucose into the film. This means that the accompanying activity of the enzyme resulted in a nonnegligible thickness change (as in the case if it were just nonspecific adsorption on the surface) because of the incorporation of glucose into the film. On the basis of modeling with *WINSPALL*, this thickness change is about 5 nm. To verify this digestion by the enzyme, direct SPR/amperometric measurements were followed with the incremental addition of glucose. Figure 10 shows simultaneous observation of the SPR reflectivity and current changes upon the successive addition of 10 mM glucose. Both the reflectivity and current increased when increments of 10 mM glucose were added into the buffer solution. This stepwise increase in the current and reflectivity indicates that glucose is continually "sensed" without blockage or nonspecific adsorption on the surface, although no saturation experiments were performed. This may well contain some pairing of the buffer ions (chloride and phosphonate) on the conducting polymer (7, 8) because the enzyme activity leads to a greater oxidized state of the conducting polymers (doping). In general, these films were very robust during the whole duration of these experiments. Further long-term stability studies may be necessary for evaluating their practical device applications.

CONCLUSION

In this work, we have demonstrated the feasibility and practical aspect of utilizing EC-SPR and waveguide mode spectroscopy for glucose sensing using a water-soluble N-alkylaminated polypyrrole as mediating layers in a composite GO_x enzyme electrode. The fact that the LbL electrostatic assembly technique can be utilized indicates the versatility of the process and the ease of future preparation for other enzymes and conducting polymers. The electrochemical and optical signals were obtained from the composite LbL enzyme electrode upon the addition of glucose because the electroactivity and electrochromic property of the polypyrrole film (absent with the PDADMAC layer) enhanced signaling. This was essentially due to the doping−dedoping activity of the polypyrrole mediator. Furthermore, the use of an EC-SPR/waveguide setup was found to be key in distinguishing the enzymatic activity from changes in the film thickness and the subphase dielectric constant. This enabled the real-time optical signal change to be separated from the change of the dielectric constant of the enzyme layer and the changes from nonenzymatic reactions such as adsorption of glucose and a change of the refractive index of the solution. This was done by analyzing both the SPR mode and the $m = 0$ and 1 modes of the waveguide in SPR/waveguide spectroscopy at various parameters and comparing their modeled behavior. In the future, this protocol should be useful for other types of enzymatic-based sensors.

Acknowledgment. The authors gratefully acknowledge partial funding from the National Science Foundation (Grant ARRA-CBET-0854979) and Robert A. Welch Foundation (Grant E-1551). A.B. acknowledges an NIH Keck Center Nanobiology Fellowship (NIH Grant 3 R90 DK071504-03). R.C.A. acknowledges previous support for visits to the AIT with W.K.

Supporting Information Available: Schematic diagrams, spectroelectrochemistry, EC-SPR of multilayers, modeling, synthesis procedure details, and ^{1}H NMR spectra. This material is available free of charge via the Internet at http://pubs.acs.org.

REFERENCES AND NOTES

(1) Wang, D.; Gong, X.; Heeger, P. S.; Rininsland, F.; Bazan, G. C.; Heeger, A. J. *Proc. Natl. Acad. Sci. U.S.A.* **2002**, *99*, 49.
(2) Peter, K.; Nilsson, R.; Inganäs, O. *Nat. Mater.* **2003**, *2*, 419.
(3) Wallace, G. G.; Kane-Maguire, L. A. P. *Adv. Mater.* **2002**, *14*, 953.
(4) Kros, A.; Hövell, S.; Sommerdijk, N.; Nolte, R. *Adv. Mater.* **2002**, *13*, 1555.
(5) Baba, A.; Advincula, R. C.; Knoll, W. In *Novel Methods to Study Interfacial Layers*; Möbius, D., Miller, R., Eds.; Studies in Interface Science Series; Elsevier Science: New York, 2001; Vol. 11, p 55.
(6) Raitman, O.; Katz, E.; Willner, I.; Chegel, V.; Popova, G. *Angew. Chem., Int. Ed.* **2001**, *40*, 3649.
(7) Baba, A.; Advincula, R. C.; Knoll, W. *J. Phys. Chem. B* **2002**, *106*, 1581.

(8) Baba, A.; Park, M.-K.; Advincula, R. C.; Knoll, W. *Langmuir* **2002**, *18*, 4648.
(9) Chegel, V.; Raitman, O.; Katz, E.; Gabai, R.; Willner, I. *Chem. Commun.* **2001**, 883.
(10) Kang, X.; Jin, Y.; Chen, G.; Dong, S. *Langmuir* **2002**, *18*, 1713.
(11) Baba, A.; Knoll, W.; Advincula, R. *Rev. Sci. Instrum.* **2006**, *77*, 064101.
(12) Calvo, E. J.; Forzani, E.; Tero, M. *J. Electroanal. Chem.* **2002**, *538–539*, 231.
(13) (a) Raitman, O.; Katz, E.; Bückmann, A. F.; Willner, I. *J. Am. Chem. Soc.* **2002**, *124*, 6478. (b) Hsieh, H.; Pfeiffer, Z.; Amiss, T.; Sherman, D.; Pitner, B. *Biosens. Bioelectron.* **2004**, *19*, 653. (c) Iwasaki, Y.; Horiuchi, T.; Niwa, O. *Anal. Chem.* **2001**, *73*, 1595. (d) Lam, W.; Chua, L.; Wong, C.; Zhang, Y. *Sens. Actuators, B* **2005**, *105*, 138.
(14) (a) Hodak, J.; Etchenique, R.; Calvo, E. J.; Singhal, K.; Bartlett, P. N. *Langmuir* **1997**, *13*, 2708. (b) Constantine, C. A.; Gattás-Asfura, K. M.; Mello, S. V.; Crespo, G.; Rastogi, V.; Cheng, T. C.; DeFrank, J. J.; Leblanc, R. M. *Langmuir* **2003**, *19*, 9863. (c) Ferreira, M.; Fiorito, P. A.; Oliveira, O. N.; Torresi, S. I. C. *Biosens. Bioelectron.* **2004**, *19*, 1611.
(15) (a) Yasuzawa, M.; Kunugi, A. *Electrochem. Commun.* **1999**, 459–462. (b) Werner, H.; Raden, D.; Murty, D. *J. Org. Chem.* **1956**, 896–898.
(16) (a) Decher, G.; Hong, J. D. *Ber. Bunsen-Ges. Phys. Chem.* **1991**, *95*, 1430. (b) Decher, G.; Hong, J. D. *Makromol. Chem. Makromol. Symp.* **1991**, *46*, 321.
(17) Advincula, R. *IEICE Trans. Electron.* **2000**, *7*, 1104.
(18) (a) Umana, M.; Waller, J. *Anal. Chem.* **1986**, *58*, 2979–2983. (b) Bélanger, D.; Nadreau, J.; Fortier, G. *J. Electroanal. Chem.* **1989**, *274*, 143. (c) Foulds, N.; Lowe, C. *J. Chem. Soc., Faraday Trans. 1* **1986**, *82*, 1259. (d) Bélanger, D.; Fortier, G. *Biotechnol. Bioeng.* **2004**, *37*, 854. (e) Yasuzawa, M.; Nieda, T. *Sens. Actuators B* **2000**, *66*, 77.
(19) Aulasevich, A.; Roskamp, R.; Jonas, U.; Menges, B.; Dostalek, K.; Knoll, W. *Macromol. Rapid Commun.* **2009**, *30*, 872.
(20) Ram, M.; Adami, M.; Paddeu, S.; Nicolini, C. *Nanotechnology* **2000**, *11*, 112.

AM100373V